Exp Biomed Res 2025; 8(4): 291-300 **https://doi.org/ 10.30714/j-ebr.2025.258**

Experimental Biomedical Research *Original article*

Alcoholic neuropathy-associated changes in K^+ conductance of primary dorsal root ganglion neurons

Feyza Alyu Altinok[1*], Ahmed Hasan[2], Ilhem Dallali[3], Abderaouf Boubekka[2], Yusuf Ozturk[4]

[1]*Department of Pharmacology, Anadolu University, Faculty of Pharmacy, Eskisehir, Türkiye*

[2]*Department of Pharmacology, Anadolu University, Graduate School of Health Sciences, Eskisehir, Türkiye*

[3]*KU Leuven, VIB-KU Leuven Center for Brain and Disease Research and Department of Cellular and Molecular Medicine, Leuven, Belgium*

[4]*Department of Pharmacology, Istanbul Aydın University, Faculty of Pharmacy, Istanbul, Türkiye*

ABSTRACT

Aim: Alcohol-induced peripheral neuropathy (AIN) is a prevalent and debilitating condition, yet current knowledge of the molecular mechanisms is limited. In this study, we aimed to analyze the impact of chronic alcohol exposure on macroscopic K^+ currents in dorsal root ganglion (DRG) neurons, providing insight into potential therapeutic targets for neuropathic pain.

Methods: An AIN model was established in adult male Sprague-Dawley rats by administering 35% ethanol (10 g/kg, twice daily) for 10 weeks. Whole-cell patch-clamp methodology was applied to measure macroscopic outward K^+ currents in the DRG. Depolarizing voltage steps (−60 to +100 mV, 10 mV increments) were applied to elicit K^+ currents. Data were analyzed for current–voltage relationships, conductance–voltage curves, and steady-state activation parameters (maximum conductance, half-activation voltage $V_{1/2}$, and slope factor *k*).

Results: Electrophysiological recordings revealed that peak K^+ current amplitudes in DRG neurons were significantly reduced in AIN rats (7.6 ± 0.7 nA) compared to controls (10.2 ± 0.7 nA, $p < 0.05$) at voltages between + 80 and + 100 mV. Maximum K^+ conductance was also decreased in the AIN group (42.2 ± 3.9) versus controls (56.1 ± 4.1, $p < 0.05$). Additionally, $V_{1/2}$ shifted leftward in AIN neurons (1.6 ± 1.9 mV) compared to controls (9.4 ± 2.1 mV), and the slope factor (*k*) modestly changed from 17.7 ± 1.2 to 20.7 ± 1.1.

Conclusion: By elucidating a key ionic mechanism underlying alcohol-induced neuropathy, this study provides a strong foundation for the development of targeted pharmacotherapies aimed at restoring K^+ channel function for AIN.

Keywords: Alcohol-induced neuropathy, dorsal root ganglion, K^+ currents, patch clamp technique.

✉ *Feyza Alyu Altinok**

Department of Pharmacology, Anadolu University, Faculty of Pharmacy, Eskisehir, Türkiye

E-mail: feyzaalyu@anadolu.edu.tr

Received: 2025-07-08 / Revisions: 2025-08-06

Accepted: 2025-08-13 / Published: 2025-09-15

1. Introduction

The development of alcohol-induced neuropathy (AIN) has been associated with abnormalities in peripheral sensory neurons [1]. Chronic alcohol intake is recognized as a significant contributor to peripheral

neuropathy, a disorder often marked by distressing symptoms, such as mechanical allodynia and thermal hyperalgesia [2]. AIN is common and clinically significant [3], yet its cellular and molecular mechanisms remain poorly understood. While research on AIN is still limited, expanding our knowledge of the underlying mechanisms is crucial for enhancing current clinical management approaches and holds promise for the development of innovative, potentially curative therapies in the future.

Notably, dorsal root ganglion (DRG) neurons—critical hubs for processing and relaying nociceptive information—are implicated in the pathophysiology of numerous neuropathic pain states [4-5]. In the present study, a rat model of chronic alcohol administration was utilized to induce neuropathy, employing a regimen of twice-daily alcohol exposure over a period of 10 weeks [6]. The establishment of neuropathic pain was confirmed through behavioral assessments, including the electronic von Frey test for mechanical allodynia and the Hargreaves test for thermal hyperalgesia. Subsequently, DRG neurons were isolated to investigate the impact of prolonged alcohol intake on macroscopic K^+ currents. Functional alterations in outward K^+ currents, key determinants of neuronal excitability, were assessed using whole-cell patch-clamp electrophysiology [7]. In this study, we aimed to analyze the impact of chronic alcohol exposure on macroscopic K^+ currents in dorsal root ganglion (DRG) neurons, providing insight into potential therapeutic targets for neuropathic pain.

2. Materials and methods

2.1. Ethics statement and experimental animals: All procedures were conducted in accordance with the guidelines established by the National Institutes of Health for the care and use of laboratory animals (NIH Publication No. 80-23, revised 1978) and fully complied with the requirements of the EU Directive 2010/63/EU on the protection of animals used for scientific purposes. Ethical approval for the experimental protocol was obtained from the Anadolu University Local Ethics Committee (Decision No: 2021-47). The experimental model consisted of male Sprague-Dawley rats with a weight range of 250–300 g and an age of 8–12 weeks. Animals were group-housed (maximum five per cage) under standard laboratory conditions, with ad libitum access to food and water. Procedures were performed within the timeframe of 10:00–16:00.

2.2. Experimental paradigm for the AIN model: A well-established protocol involving the oral administration of ethanol (35% v/v, 10 g/kg, twice daily) over a period of 10 weeks has been shown to induce hyperalgesia and allodynia in rats [8]. In the present study, the alcoholic neuropathy model was established in adult male Sprague-Dawley rats of comparable age and body weight (200–250 g) by administering 35% v/v ethanol, prepared in double-distilled water at a dose of 10 g/kg twice daily via gavage for a duration of 10 weeks (n = 8). The control animals received an equivalent volume of distilled water following the same administration schedule [9-10].

2.3. Chemicals: Ethyl alcohol (pure, ≥99.5%) and phosphate-buffered saline (PBS) were purchased from Sigma-Aldrich (St. Louis, MO, USA). All salts used in the preparation of internal and external recording solutions, along with trypsin, were sourced from Multicell (Wisent Inc., St. Bruno, Quebec, Canada). Collagenase type IV and Dulbecco's Modified Eagle Medium (DMEM) were purchased from Gibco (Life Technologies, Carlsbad, CA,

USA). EGTA was obtained from Biomatik (Cambridge, Ontario, Canada), and ATP was supplied by Genaxxon Bioscience (Biberach an der Riß, Germany).

2.4. Determination of neuropathic pain: Mechanical sensitivity was assessed using an electronic von Frey device (Ugo Basile, Model 38450, Varese, Italy). Rats were individually placed in Plexiglas enclosures (17 × 69 × 14 cm^3) on an elevated wire mesh and allowed to acclimate for 15–30 minutes. A stainless steel probe was applied perpendicularly to the right hind paw, with force gradually increased until a withdrawal reflex occurred. The device automatically recorded the paw withdrawal threshold (PWT, gf). Three measurements were taken at five-minute intervals, and the mean was calculated. A cut-off of 50 gf was set to prevent injury [11].

Thermal sensitivity was evaluated using the Hargreaves test (Ugo Basile, Model 37370, Varese, Italy). After a 15–30 minute acclimation in identical Plexiglas chambers on a glass platform, a focused heat source was applied to the midplantar surface of the left hind paw. The timer stopped upon withdrawal or at a 30-second cut-off to avoid burns. Paw withdrawal latency (PWL) was recorded automatically. Three trials were performed per rat at 5-minute intervals, and the average was used for analysis [12].

2.5. Isolation and culture of primary DRG neurons: DRG neurons were isolated and cultured in accordance with a protocol previously established [13]. In brief, anesthetic induction was performed using ketamine (90 mg/kg) plus xylazine (10 mg/kg) via intraperitoneal route at a total injection volume of 1 mL/kg, followed by swift decapitation. The vertebral columns were excised and promptly immersed in ice-cold PBS. The DRGs were meticulously dissected and transferred into ice-cold DMEM. Using fine surgical instruments, including a scalpel and iris scissors, extraneous connective tissue and debris were carefully removed from the ganglia.

The cleaned DRGs were enzymatically digested at 37 °C in an atmosphere of 5% CO_2 for 45 minutes in DMEM containing 1× Penicillin/Streptomycin and 2 mg/mL collagenase type IV (Sigma). Enzymatic activity was terminated by rinsing the tissue three times with PBS. Subsequently, the ganglia were incubated for an additional 7 minutes in 1 mL of DMEM supplemented with 1× Penicillin/Streptomycin and 100 µL of 0.25% trypsin (1:250; Sigma). Trypsin was then removed through repeated washes with fresh DMEM.

Following the final wash, 4 mL of complete culture medium (DMEM supplemented with 1× Penicillin/Streptomycin and fetal bovine serum) was added. The ganglia was gently triturated using a 1000 µL pipette tip to yield a single-cell suspension. This suspension was plated onto glass petri dishes and maintained at 37 °C in 5% CO_2. Patch-clamp recordings were initiated 1–2 hours after dissociation to permit neuronal recovery from enzymatic and mechanical processing.

2.6. The process and protocol for electrophysiology: Recordings in the whole-cell patch-clamp configuration were performed at room temperature (18–20 °C) employing standard electrophysiological techniques. Patch pipettes were pulled from borosilicate glass capillaries with internal filaments (Sutter Instrument, BF150-110–10) using a P-97 Micropipette Puller (Sutter Instrument), yielding electrodes with resistances between 2 and 5 MΩ. High-resistance seals (in the GΩ range) were formed by applying gentle negative pressure, either manually (mouth suction) or with a 1 mL syringe. Transition to the whole-

cell configuration was confirmed by the presence of capacitive transients, a substantial reduction in access resistance, and a decrease in membrane resistance from the GΩ range to approximately 500 MΩ. Recordings were performed using a Sutter Integrated Patch Amplifier (IPA) with a single headstage, operated in voltage-clamp mode, and controlled via SutterPatch® Data Acquisition Software (v2.0.4, Windows® 10). Currents were digitized at 25 kHz and low-pass filtered at 5 kHz using the amplifier's internal filter. Pipette capacitance and series resistance were automatically compensated for. All data acquisition and analyses were carried out within the SutterPatch software environment.

Neurons were initially held at a membrane potential of −60 mV, followed by 300 ms step depolarizations to 0 mV, which were repeated until stable outward currents were obtained. The test protocol was introduced only after the current stability was verified. Current–voltage (I–V) relationships were then generated by applying a series of depolarizing pulses from −60 mV to + 100 mV in 10 mV increments, each delivered from a holding potential of −60 mV to activate voltage-gated K^+ channels.

The internal solution contained (in mM): NaCl 10, KCl 140, EGTA 1.1, $CaCl_2$ 0.1, HEPES Acid 10, $MgCl_2$ 2, D-glucose 3, and pH was adjusted to 7.2 with KOH. The external solution contained (in mM): $MgCl_2$ 1, NaCl 140, KCl 3, $CaCl_2$ 1, HEPES Acid 10, D-glucose 10, and the pH titrated to 7.3 with NaOH.

K^+ channel activation was investigated by the conductance through transformation of the peak current–voltage (I–V) data. Conductance (G) at each test potential was calculated from the peak current (I) using the equation: $G = I / (V - V_{rev})$, where V is the membrane potential at which current was recorded, and V_{rev} is the reversal potential, determined to be −82 mV for the internal and external K^+ by using the Nernst equation. The G values were fitted by a Boltzmann equation: $y = A_2 + (A_1-A_2)/ (1 + \exp(x-x_0)/dx))$ where y is conductance, A_1 is the value at the low asymptote; A_2 is the value at the high asymptote; x_0 is the midpoint (value of x at half-maximal response ($V_{1/2}$)) and dx is the slope factor (*k*).

2.7. Statistical Analysis: Statistical evaluations were carried out using GraphPad Prism (v10.0.2) and OriginPro 2021 (64-bit, v9.8.0.200, Learning Edition). The progression of neuropathic pain was evaluated with a paired Student's *t*-test, while differences between groups in the electrophysiological experiments were analyzed using an unpaired Student's *t*-test. A p-value of less than 0.05 was considered indicative of statistical significance. Results are shown as mean ± standard error of the mean (SEM).

4. Results

3.1. Development of Neuropathic Pain: Figure 1 depicts the alterations in mechanical and thermal sensitivity observed after 10 weeks of ethanol administration, assessed with e-Von Frey and Hargreave's tests, respectively. As expected, both mechanical and thermal thresholds were markedly decreased in the ethanol-treated group at week 10 relative to baseline values recorded on day 0 (***$p < 0.001$, n = 8), consistent with the induction of neuropathic pain.

3.2. AIN pathology alters the K^+ channel current dynamics: To assess the impact of AIN on K^+ currents, whole-cell voltage-clamp recordings were performed on small- and medium-sized DRG neurons (membrane capacitance ≤35 pF). Steady-state activation is a key characteristic of K^+ currents and plays a vital role in regulating the excitability of DRG neurons. To explore this, we examined the

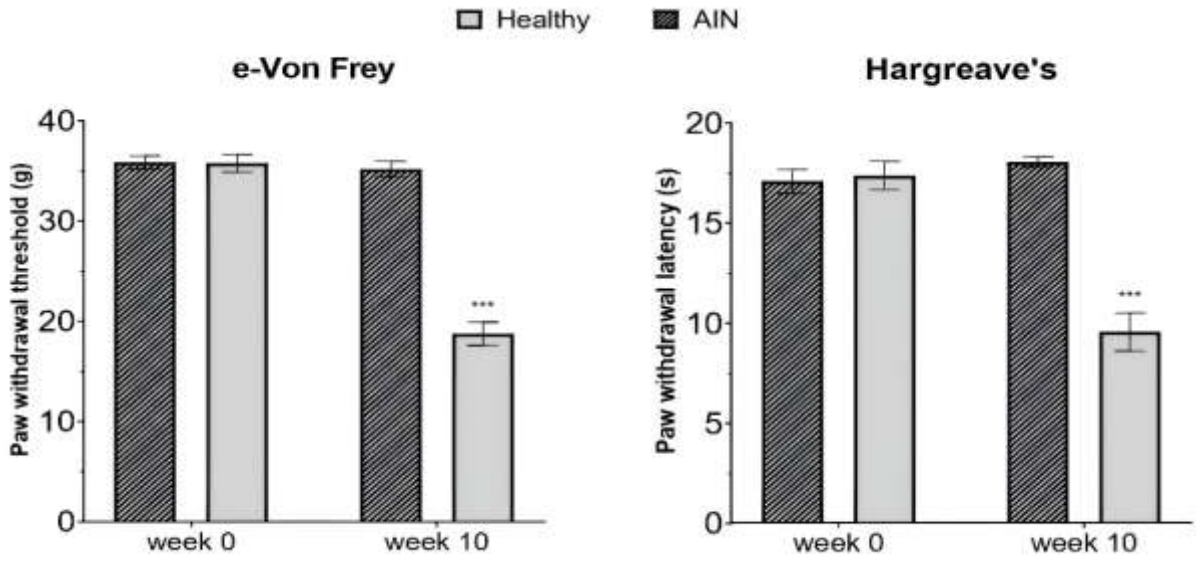

Figure 1. Changes in mechanical and thermal thresholds between the 0th and 10th weeks in the experimental groups. $^{***}p < 0.001$ indicates a statistically significant difference in the ethanol-administered group compared to its own baseline values at day 0. Paired Student's *t* test was conducted using mean ± S.E.M. values (n=8).

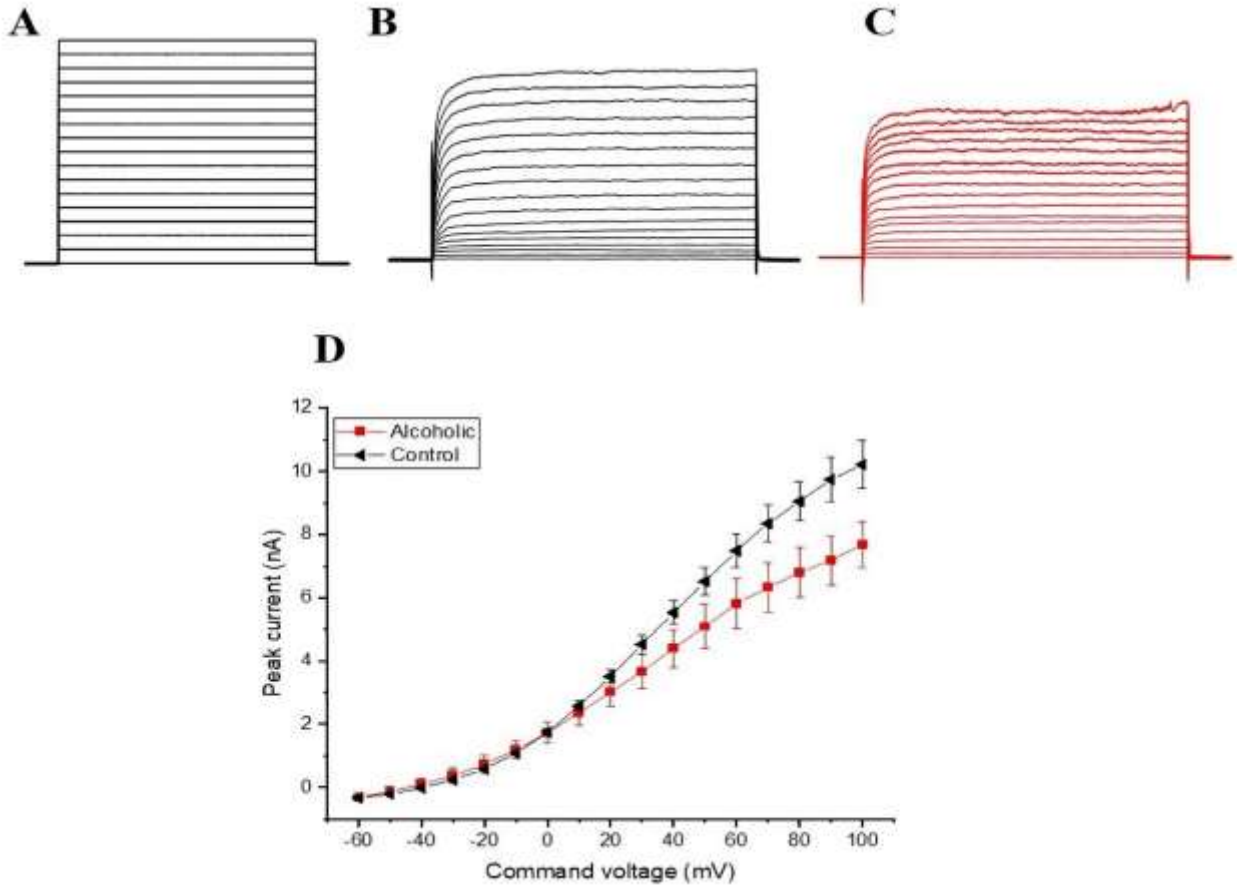

Figure 2. Electrophysiological characterization of macroscopic K^+ currents in DRG neurons from AIN and Control groups. (A) Voltage-step protocol applied from a holding potential of –60 mV to + 100 mV in 10 mV increments. (B) Representative current traces recorded from Control DRG neurons. (C) Representative current traces recorded from the AIN DRG neurons. (D) Steady-state current-voltage (I–V) relationship of K^+ currents in both groups. Data are presented as mean ± S.E.M. (n = 15 for control and n = 8 for AIN). Statistical analysis was performed using an unpaired Student's *t*-test.

steady-state current–voltage (I–V) relationship of macroscopic K^+ currents in DRG neurons. Our results revealed a significant depolarizing shift in K^+ currents in DRG neurons from AIN rats compared to controls (Figure 2D; Control: 10.2 ± 0.7 nA vs. AIN: 7.6 ± 0.7 nA, $p < 0.05$ for voltage range of 80-100 mV). Additionally, there was a marked reduction in the amplitude of K^+ activation current traces in the AIN neurons (Figures 2B and 2 C), indicating altered channel function associated with AIN.

As shown in Figure 3, the values of $V_{1/2}$ for activation of total K^+ current in control and in AIN cells were 9.4 ± 2.1 and 1.6 ± 1.8 mV (n = 8, $p < 0.05$), respectively. Conversely, the slope factor *k* slightly changed but did not show significant variation between the control group (17.7 ± 1.2 mV) and AIN DRGs (20.7 ± 1.1 mV, n = 8, $p < 0.05$). Thus, AIN pathology produced a -7.8 ± 0.3 mV hyperpolarized shift in the $V_{1/2}$ of the steady-state activation curve. To summarize, AIN was shown to significantly reduce the maximum conductance and shift the voltage for half-maximal activation ($V_{1/2}$) to a more negative value, indicating modified channel-gating properties in such a way as to induce hyperexcitability.

Figure 4 provides the outcome that AIN DRG neurons present a significantly high decrease in the K^+ current densities ($^{***}p < 0.001$). The macroscopic K^+ current density was determined by dividing the current amplitude (pA) by the membrane capacitance (pF) of the recorded DRG neurons. The observed changes collectively suggest enhanced neuronal excitability following AIN.

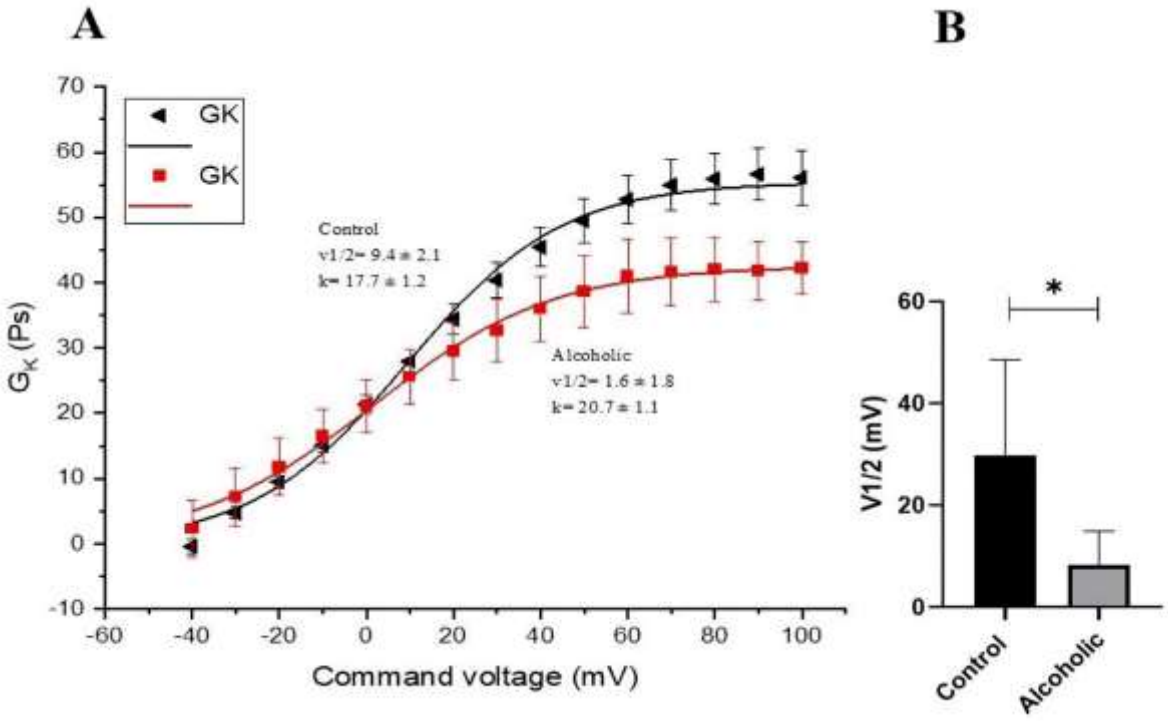

Figure 3. Conductance–voltage (G–V) relationship in the control and AIN groups. (A) conductance–voltage curves recorded from DRG neurons of control (black rectangle) and AIN (red squares) rats. Data are presented as mean ± S.E.M. (n = 8 per group) The G–V curves were fitted using a Boltzmann function, yielding the following parameters: Control: Maximum conductance = 56.1 ± 4.1, $V_{1/2}$ = 9.4 ± 2.1 mV, slope factor (*k*) = 17.7 ± 1.2, AIN: Maximum conductance = 42.2 ± 3.9, $V_{1/2}$ = 1.6 ± 1.8 mV, *k* = 20.7 ± 1.1. A significant leftward shift in $V_{1/2}$ was observed in the AIN group compared to the control group (*$p < 0.05$), indicating enhanced voltage sensitivity and altered channel gating dynamics.

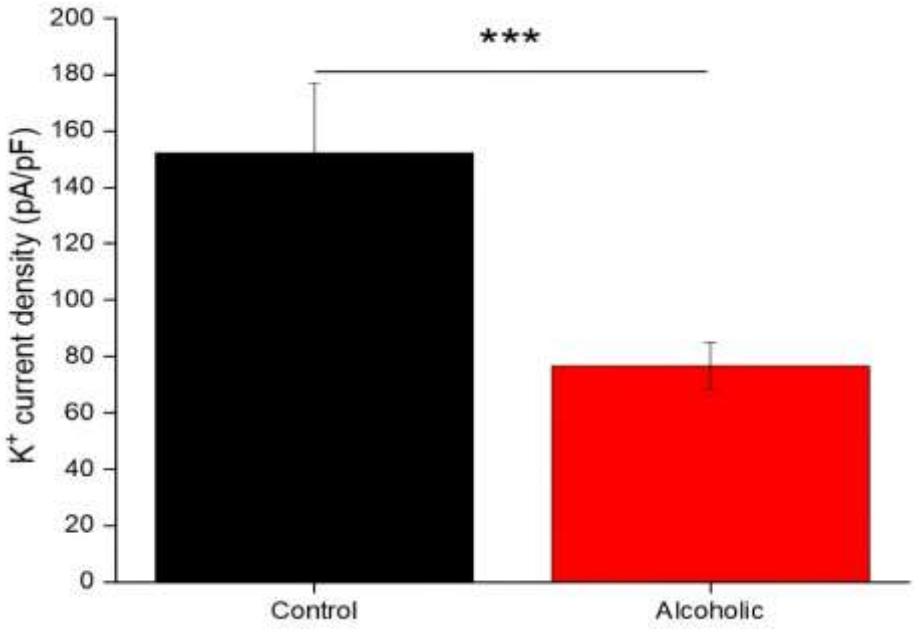

Figure 4. Summary of the K^+ current density from healthy control and AIN rat DRG neurons. ***p < 0.001; significance between AIN versus healthy control DRG neurons. Unpaired Student's *t*-tests were applied using ± S.E.M. values (n = 10 per group).

4. Discussion

K^+ currents are crucial for the repolarization phase of the action potential, which restores the membrane potential to the baseline after depolarization. A reduction in these currents delays repolarization, broadens action potentials, and typically enhances neuronal excitability due to the prolonged depolarized state that facilitates repetitive firing [14]. This repolarization is primarily mediated by voltage-gated K^+ channels that open more slowly than Na^+ channels but remain open longer, allowing K^+ efflux that brings the membrane potential back toward the negative resting level. The slow deactivation of these channels also causes the after hyperpolarization phase, which temporarily makes the neuron less excitable.

In the present study, the AIN model exhibited a marked decrease in both the peak amplitudes (Figure 2) and current densities (Figure 4) of K^+ currents in primary DRG neurons, particularly within the depolarized voltage range of + 40 to + 100 mV. In the AIN model, the observed reduction in peak amplitudes and current densities of K^+ currents, especially at depolarized voltages (+ 40 to + 100 mV), suggests an impaired ability of neurons to repolarize efficiently. This likely compromises the action potential repolarization, contributing to the hyperexcitable phenotype observed. This leads to broadened action potentials and a prolonged depolarized state, which facilitates repetitive firing and increased neuronal excitability, a hallmark of neuropathic pain states. Such changes in K^+ channel function can disrupt the delicate balance of ionic conductances that regulate excitability and firing patterns.

Further analysis of the steady-state activation properties revealed notable alterations (Figure 3). In the control neurons, the maximum conductance was 56.1 ± 4.1, with a half-activation voltage ($V_{1/2}$) of 9.4 ± 2.1 and a slope factor (k) of 17.7 ± 1.2. Neurons from the AIN group demonstrated a reduced maximum conductance of 42.2 ± 3.9 and a significant leftward shift in achieve comparable

channel activation. The shift in steady-state activation properties—a reduced maximum conductance and a leftward shift in voltage dependence—indicates that K^+ channels in AIN neurons activate at more hyperpolarized potentials but with less maximal current.

The slope factor showed a modest decrease to 20.7 ± 1.1, which, although not statistically significant, suggests a slightly steeper voltage dependence of activation. A reduced *k* implies increased voltage sensitivity, where small changes near $V_{1/2}$ result in larger alterations in channel conductance. However, this sharper activation does not compensate for the overall reduction in maximum conductance. Although a steeper voltage dependence (reduced slope factor) might suggest increased sensitivity, it does not compensate for the overall loss of K^+ current amplitude. This altered gating likely contributes further to abnormal excitability by changing the timing and extent of K^+ efflux during action potentials.

From a pathophysiological perspective, diminished K^+ currents are well known to enhance neuronal excitability and promote pain hypersensitivity. Conversely, increased K^+ channel activity generally has antinociceptive effects by stabilizing membrane potential and limiting excessive firing [7]. Our whole-cell patch-clamp recordings underscore the functional impact of chronic alcohol exposure on K^+ channel dynamics, supporting the notion that modulation of these currents directly influences nociceptive processing within the AIN.

Moreover, the specific types of K^+ channels are involved in repolarization, such as Kv subfamilies, and each has distinct kinetics and voltage dependencies that shape action potential duration and firing frequency. Alterations in these channel subtypes could affect neuronal signaling d. For example, Kv3 channels enable high-frequency firing due to their rapid activation and deactivation, and their dysfunction could impair normal firing patterns critical for sensory processing. In addition, observations that Kcnq expression is associated with alcohol intake and that retigabine lowers consumption indicate that KV7 channels may serve as pharmacogenetic targets for treating alcohol use disorder related conditions [15].

Therapeutically, these findings highlight K^+ channels as promising targets for intervention in AIN. Pharmacological agents, such as flupirtine (used in Europe for pain), that enhance K^+ channel activity or restore normal gating properties could potentially reduce neuronal hyperexcitability and alleviate neuropathic pain symptoms. Despite some limitations related to side effects observed with agents like retigabine (discontinued clinically due to side effects), novel modulators with improved safety profiles are under investigation and could offer targeted relief for AIN patients. Additionally, neuronal K^+ channel openers, such as retigabine and flupirtine, have been reported to reduce alcohol consumption in rats [16-18], offering dual benefits in the context of AIN. Topiramate has been shown to facilitate K^+ conductance and several studies suggest a role for topiramate in treating alcohol use disorders. SK channels, a class of small-conductance calcium-activated K^+ channels, have been proposed in recent works as a novel approach to alcoholism treatment [19-20]. Future studies could focus on identifying which K^+ channel subtypes are most affected in AIN and testing modulators that selectively target these channels to develop more effective treatments.

In summary, this study provides novel evidence that the AIN model induces substantial reductions in macroscopic K^+

currents in DRG neurons, which likely underpins the behav development of mechanical allodynia and thermal hyperalgesia observed. These findings not only advance our understanding of the pathophysiological mechanisms driving AIN, but also highlight K^+ channels as promising therapeutic targets. Pharmacological targeting of these channels holds promise for new experimental treatments for AIN through modulation of excitability and pain.

4.1 Conclusion: In conclusion, this study provides electrophysiological evidence that chronic alcohol exposure impairs K^+ channel function in DRG neurons, leading to disrupted repolarization and heightened neuronal excitability. These findings deepen our understanding of the molecular mechanisms underlying AIN and highlight K^+ channels as promising therapeutic targets to alleviate the pain hypersensitivity associated with this condition. Importantly, our work establishes a critical foundation for translational research by highlighting a specific molecular dysfunction within the complex pathophysiology of AIN. By illuminating some key ionic mechanisms, this research paves the way for innovative treatments designed to restore neuronal function and improve clinical outcomes in patients suffering from AIN.

Funding: *This work has been supported financially by the Anadolu University Research Foundation (Eskisehir, Türkiye), Project no: 2211S207 and 2203S022.*

Conflict of Interest: *The authors declared no conflict of interest.*

Ethical Statement: *The experimental protocol was approved by the Anadolu University Local Ethics Committee (Decision No: 2021-47).*

References

[1]Chopra K, Tiwari V. Alcoholic neuropathy: possible mechanisms and future treatment possibilities. Br J Clin Pharmacol. 2012;73(3):348-362.

[2]Borgonetti V, Roberts AJ, Bajo M, Galeotti N, Roberto M. Chronic alcohol induced mechanical allodynia by promoting neuroinflammation: A mouse model of alcohol-evoked neuropathic pain. Br J Pharmacol. 2023;180(18):2377-2392.

[3]Julian T, Glascow N, Syeed R, Zis P. Alcohol-related peripheral neuropathy: A systematic review and meta-analysis. J Neurol. 2019;266(12):2907-2919.

[4]Abd-Elsayed A, Vardhan S, Aggarwal A, Vardhan M, Diwan SA. Mechanisms of action of dorsal root ganglion stimulation. Int J Mol Sci. 2024;25(7):3591.

[5]Djouhri L, Zeidan A, Abd El-Aleem SA. Changes in expression of Kv7.5 and Kv7.2 channels in dorsal root ganglion neurons in the streptozotocin rat model of painful diabetic neuropathy. Neurosci Lett. 2020;736:135277.

[6]Kandhare AD, Ghosh P, Ghule AE, Bodhankar SL. Elucidation of molecular

mechanism involved in neuroprotective effect of Coenzyme Q10 in alcohol-induced neuropathic pain. Fundam Clin Pharmacol. 2013;27(6):603-622.

[7] Du X, Gamper N. Potassium channels in peripheral pain pathways: Expression, function and therapeutic potential. Curr Neuropharmacol. 2013;11(6):621-640.

[8] Kandhare AD, Raygude KS, Ghosh P, Ghule AE, Bodhankar SL. Therapeutic role of curcumin in prevention of biochemical and behavioral aberration induced by alcoholic neuropathy in laboratory animals. Neurosci Lett. 2012;511(1):18-22.

[9] Tiwari V, Kuhad A, Chopra K. Tocotrienol ameliorates behavioral and biochemical alterations in the rat model of alcoholic neuropathy. Pain. 2009;145(1):129-135.

[10] Kaur M, Singh A, Kumar B, et al. Protective effect of co-administration of curcumin and sildenafil in alcohol induced neuropathy in rats. Eur J Pharmacol. 2017;805:58-66.

[11] Spradley JM, Guindon J, Hohmann AG. Inhibitors of monoacylglycerol lipase, fatty-acid amide hydrolase and endocannabinoid transport differentially suppress capsaicin-induced behavioral sensitization through peripheral endocannabinoid mechanisms. Pharmacol Res. 2010;62(3):249-258.

[12] Chen KH, Yang CH, Wallace CG, et al. Combination therapy with extracorporeal shock wave and melatonin markedly attenuated neuropathic pain in rat. Am J Transl Res. 2017;9(10):4593.

[13] Altinok FA, Dallali I, Boubekka A, Hasan A, Ozturk Y. Optimized primary dorsal root ganglion cell culture protocol for reliable K^+ current patch-clamp recordings. Neurosci Lett. 2025;844:138038.

[14] Blaine JT, Ribera AB. Kv2 channels form delayed-rectifier potassium channels in situ. J Neurosci. 2001;21(5):1473-1480.

[15] Rinker JA, Fulmer DB, Trantham-Davidson H, Smith ML, Williams RW, Lopez MF et al. Differential potassium channel gene regulation in BXD mice reveals novel targets for pharmacogenetic therapies to reduce heavy alcohol drinking. Alcohol. 2017;58:33-45.

[16] Knapp CM, O'Malley M, Datta S, Ciraulo DA. The Kv7 potassium channel activator retigabine decreases alcohol consumption in rats. Am J Drug Alcohol Abuse. 2014;40(3):244-250.

[17] Aliyev NA, Aliyev Z. Neuronal Potassium Channel Openers Flupirtine (SNEPCO) in the Treatment of the Alcohol Withdrawal without Psy-chiatric Comorbidity Randomized, Double-Blind, Placebo-Controlled Study. J Addict Addictv Disord. 2017;4:013.

[18] Zwierzyńska E, Andrzejczak D, Pietrzak B. Does retigabine affect the development of alcohol dependence?—A pharmaco-EEG study. Neurosci. Lett. 2016;611:6-13.

[19] Addolorato G, Leggio L, Hopf FW, Diana M, Bonci A. Novel therapeutic strategies for alcohol and drug addiction: focus on GABA, ion channels and transcranial magnetic stimulation. Neuropsychopharmacol. 2012;37(1):163-177.

[20] Johnson BA, Ait-Daoud N, Bowden CL, DiClemente CC, Roache JD, Lawson K et al. Oral topiramate for treatment of alcohol dependence: a randomised controlled trial. The Lancet. 2003;361(9370):1677-1685.